Series of Concentration-Induced Phase Transitions in Cholesterol/Phosphatidylcholine Mixtures

István P. Sugár,[†][*] István Simon,[‡] and Parkson L.-G. Chong[§]

[†]Department of Neurology and Center for Translational Systems Biology, Icahn School of Medicine at Mount Sinai, New York, New York; [‡]Institute of Enzymology, Research Center for Natural Sciences, Hungarian Academy of Sciences, Budapest, Hungary; and [§]Department of Biochemistry, Temple University School of Medicine, Philadelphia, Pennsylvania

ABSTRACT   In lipid membranes, temperature-induced transition from gel-to-fluid phase increases the lateral diffusion of the lipid molecules by three orders of magnitude. In cell membranes, a similar phase change may trigger the communication between the membrane components. Here concentration-induced phase transition properties of our recently developed statistical mechanical model of cholesterol/phospholipid mixtures are investigated. A slight ($<$1%) decrease in the model parameter values, controlling the lateral interaction energies, reveals the existence of a series of first- or second-order phase transitions. By weakening the lateral interactions first, the proportion of the ordered (i.e., superlattice) phase (A_{reg}) is slightly and continuously decreasing at every cholesterol mole fraction. Then sudden decreases in A_{reg} appear at the 0.18–0.26 range of cholesterol mole fractions. We point out that the sudden changes in A_{reg} represent first- or second-order concentration-induced phase transitions from fluid to superlattice and from superlattice to fluid phase. Sudden changes like these were detected in our previous experiments at 0.2, 0.222, and 0.25 sterol mole fractions in ergosterol/DMPC mixtures. By further decreasing the lateral interactions, the fluid phase will dominate throughout the 0.18–0.26 interval, whereas outside this interval sudden increases in A_{reg} may appear. Lipid composition-induced phase transitions as specified here should have far more important biological implications than temperature- or pressure-induced phase transitions. This is the case because temperature and pressure in cell membranes are largely invariant under physiological conditions.

INTRODUCTION

Phase behavior of cholesterol and phosphatidylcholine (PC) assemblies has been extensively studied. Two phase diagrams have been frequently cited:

The first phase diagram proposes that, near the transition temperature of the phospholipid component, there are three phases: liquid-disordered (l_d) at ≤ 8 mol % cholesterol; liquid-ordered (l_o) at ≥ 25 mol % cholesterol; and the phase coexistence region at intermediate mole fractions (e.g., Ipsen et al. (1)). In the l_o phase, the lipid acyl chains are ordered but the membrane lateral mobility is retained. The second phase diagram (e.g., Huang et al. (2)) proposes that, near the transition temperature of the phospholipid component, the system is in fluid phase up to ~8 mol % and then as the cholesterol mole fraction increases (from 8 to 66 mol %) the fluid phase gradually converts to l_o phase (also called LG_I region, i.e., liquid-gel type phase). In contrast to the first type of phase diagram there is no phase boundary at 25 mol %. These phase diagrams build on studies using large cholesterol increments (e.g., $>$3 mol %).

When using small sterol mole fraction increments (~0.3 mol %) and the membrane samples subject to sufficiently long incubations to reach organization equilibrium, it was found that physical and biochemical properties, such as lipid infrared signals and the membrane probe's fluorescence intensity, anisotropy, quenching rate constant,

and lifetime as well as surface enzyme activities, from a variety of sterol/phospholipid mixtures, showed maxima (or minima) at or very close to critical sterol mole fractions such as 0.20, 0.222, 0.25, 0.333, 0.40, and 0.50 (reviewed in Chong and Olsher (3), Chong et al. (4), and Somerharju et al. (5)). These biphasic changes in membrane properties at critical sterol mole fractions have been interpreted in terms of the sterol superlattice model (6,7). The sterol superlattice model proposes that the entire membrane surface is not covered by superlattices (6). At a given sterol mole fraction, superlattices (containing regularly distributed sterol molecules) always coexist with fluid areas (containing irregularly distributed sterol molecules); however, the extent of sterol superlattice reaches a local maximum at critical sterol mole fractions. It has been proposed that sterol molecules tend to be maximally separated from each other in the superlattices to minimize the exposure of the hydrophobic region of the sterol molecules to water (the umbrella effect (8)) and to reduce the deformation stress to the matrix lipid lattice caused by the rigid and bulky steroid ring (6,7,9).

Sterol/phospholipid mixtures have also been described in terms of the formation of condensed complexes between sterol (C) and phospholipid (P) (10). This model considers the reaction

$$nqC + npP \leftrightarrow C_{nq}P_{np},$$
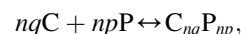
where n is the cooperativity parameter, and p and q are relatively prime numbers. The relative stoichiometry $q/(p+q)$

CrossMark

can be determined from the position of the sharp cusp in the phase diagram (10,11). The critical sterol mole fractions theoretically predicted for maximal superlattice formation coincide with the relative stoichiometries $q/(p + q)$ due to C-P complex formation. The condensed complex model has other features similar to those proposed in the sterol superlattice model. Both models contend that stability is greater and molecular order is higher at critical sterol mole fractions. Because of these similarities and the observation that the extent of sterol superlattices increases with sample incubation time (12), it has been speculated that condensed complexes and superlattices may share the same physical origin and may just occur at different times (12).

Very recently, we presented a statistical mechanical model (13) of cholesterol/phospholipid mixtures that is able to rationalize almost every critical mole fraction value previously reported for sterol superlattice formation as well as the observed biphasic changes in membrane properties at critical mole fractions. This model explains how cholesterol superlattices and cholesterol-phospholipid condensed complexes are interrelated and provides a more detailed description about the phase diagram of cholesterol/phospholipids, particularly in the LG_I region, which includes a liquid-ordered phase. According to our new theory (13), the LG_I region (8–66 mol % cholesterol) is considered to be a mixture of fluid phase (irregular regions) and aggregates of rigid clusters (regular regions). A rigid cluster is formed by a cholesterol molecule and phospholipid molecules that are condensed to the cholesterol (11). The composition of a rigid cluster agrees with a measured critical mole fraction, X_{cr}, i.e., $X_{cr} = (1 + M/2)^{-1}$ where M is the number of acyl chains condensed to the cholesterol molecule. Rigid clusters of similar size tend to aggregate. Within each aggregate of closely packed rigid clusters, the cholesterol molecules are regularly distributed into superlattices. Because the cooperativity energy of aggregation of rigid clusters w is positive and smaller than the thermal energy unit, kT (13), there are numerous aggregates with a broad size distribution (14). Furthermore, in the LG_I region (8–66 mol % cholesterol), there are a few X_{cr} values (e.g., 50.0, 40.0, 33.3, 28.6, 25.0, 22.2, 20.0, 18.2, 16.6, 15.4, 14.2, etc.) at which there is a biphasic change (reaching a maximum) in the area covered by sterol superlattices (A_{reg}) as calculated based on our statistical thermodynamics model (13) or as observed in our nystatin partition coefficient measurements (15,16). These biphasic changes in A_{reg} suggest that, within the LG_I region (including the l_o phase), multiple concentration-induced phase transitions may exist.

In this study, we further developed the statistical thermodynamics model (13) in an attempt to reveal the physical characteristics of the cholesterol mole fraction-induced phase transitions. We found a series of first- or second-order phase transitions, which are strongly dependent upon lateral interaction energies. Very small changes (e.g., 0.8%) in the lateral interaction energies, which can be triggered by physical and/or chemical perturbations, may result in considerable changes in the phase properties of the cholesterol/PC mixtures. These findings suggest that the phase behaviors of cholesterol/PC mixtures are much more complicated than previously thought.

THE MODEL

In this section, we briefly describe our recently developed statistical mechanical model of cholesterol/phospholipid mixtures (13). In our model, a monolayer of the lipid bilayer is represented by a lattice where each lattice unit is a square. There are two types of lattice units: N_s of them represent the rigid clusters (in Fig. 1 these are *solid units* with *open circle* at their center), whereas the remaining N_u lattice units represent the fluid phase of the system (in Fig. 1, these are *open units* with randomly distributed *open circles*). The surface area belonging to a lattice unit, A_M, is equal to the cross-section of a rigid cluster formed by a cholesterol and M phospholipid hydrocarbon chains condensed to the cholesterol. Rigid clusters tend to form aggregates, in which cholesterol molecules are regularly distributed into superlattices.

The Helmholtz free energy (called simply "free energy" in the rest of the article), F, of the lattice is

$$F = E_u + E_s + E_i - T\left(S_u + S_s + S_u^{mix} + S_{units}^{mix}\right), \quad (1)$$

where T is the absolute temperature. E_s and E_u are the total internal energy of the s and u state lattice units, respectively. E_i is the sum of the interaction energies between the lattice units. The lattice entropy contains four terms:

1. Total internal entropy of the u-state lattice units S_u;
2. Total internal entropy of the s-state lattice units S_s;
3. Mixing entropy of the molecules within the fluid phase S_u^{mix}; and
4. Mixing entropy of the u- and s-state lattice units S_{units}^{mix}.

These energy and entropy terms are given in Sugár and Chong (13) as a function of X_c (the cholesterol mole fraction relative to the total number of lipids in the membrane, N_{tot}) and X_c^s (the mole fraction of cholesterol situated in rigid clusters relative to the total number of lipids in the membrane). The above free energy function is valid when the mole fraction X_c is close to any of the critical cholesterol mole fractions, X_{cr}^M,

$$X_c \approx X_{cr}^M \left(= \frac{1}{1 + (M/2)} \right), \quad (2)$$

where the fundamental assumption of our model is most applicable, i.e., the system contains one type of rigid cluster, with a cluster containing $M/2$ phospholipid molecules condensed to one cholesterol molecule. Thus, according to Eq. 2, at $M = 1$, $X_{cr}^M = 0.666$, $M = 2$, $X_{cr}^M = 0.5$, etc.
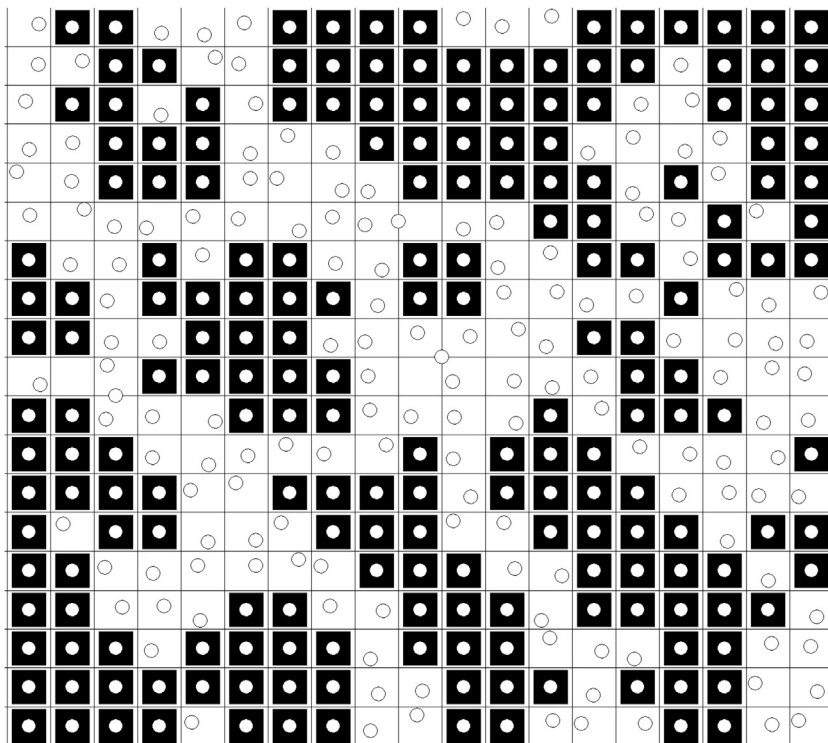
FIGURE 1 Lattice model of phospholipid/cholesterol membrane. In our recently proposed statistical mechanical model (13), a layer of the membrane is represented by a lattice where each lattice unit is a square (surrounded by *solid lines*). The surface area of a unit is equal with the surface area of a rigid cluster, A_M. A unit represents either a rigid cluster (*solid unit* with *open circle* at the center) or part of the fluid phase (*open unit* with randomly distributed *open circle*). (*Open circle*) Cholesterol. (*Solid square*) Phospholipid molecules condensed to the central cholesterol.

At any given cholesterol mole fraction, X_c, which is close to a critical mole fraction, X^M_{cr}, one can find the average number of s state lattice units, $\langle N_s \rangle = N_{tot}\langle X^s_c \rangle$. For large N_{tot}, the position of the global minimum of the free energy function (Eq. 1) well approximates the equilibrium value or the thermodynamic average of X^s_c (see maximum term approximation in Hill (17)).

RESULTS AND DISCUSSION

Table 1 in Sugár and Chong (13) lists a set of parameters of the cholesterol/phospholipid model. Using this parameter set, we have generated Fig. 2 *A* (also Fig. 3 in Sugár and Chong (13)), which shows the measured A_{reg} values at six critical mole fractions (+) and calculated A_{reg} versus X_c curves (*solid lines*). A_{reg}, the proportion of the densely packed area (i.e., proportion of s state lattice units), has been calculated by

$$A_{reg} = \frac{\langle N_s \rangle}{(\langle N_s \rangle + \langle N_u \rangle)} = \frac{\langle X^s_c \rangle}{(\langle X^s_c \rangle + \langle X^u_c \rangle)}. \quad (3)$$

Equation 4 in Sugár and Chong (13) gives X^u_c as a function of X^s_c and X_c, so A_{reg} depends solely on $\langle X^s_c \rangle$ and X_c. Regarding Fig. 2 *A*, the following two points should be emphasized:

1. The calculated A_{reg} (*solid curves*) yields a biphasic change with X_c, showing a local maximum at the respective critical mole fraction X_{cr}, similar to the A_{reg} curves

determined from nystatin partition coefficient measurements (15,16). The local maximum points of the calculated curves (*solid curves*) match with the local maxima (+) of the A_{reg} curves determined from nystatin fluorescence (15,16).

2. The lower the critical concentration X_{cr} the sharper the respective, calculated A_{reg} peak. Within a peak, A_{reg} decreases by 1–10% when $|X_c - X_{cr}| = 0.015$ but A_{reg} remains always above 0.6 (i.e., the majority of the cholesterol forms superlattice). This tendency is in general supported by the experimental results (15,16); however, in ergosterol/DMPC bilayers (15), for example, there is an extremely sharp, 60% decrease in A_{reg} within a very small change (<1 mol %) in sterol content on either side of the critical sterol mole fractions, i.e., $0.2 = X^8_{cr}$, $0.222 = X^7_{cr}$, and $0.25 = X^6_{cr}$.

In this work, we explore whether our model is capable of producing such an experimentally detected extremely sharp change. In Sugár and Chong (13), we fitted four model parameters to obtain the local maxima of the A_{reg} curves and the phase boundary between the fluid and ordered phase, in agreement with the experimental findings. The values e_{uu} and e_{us}, are the model parameters characterizing the interaction energies per unit length between nearest-neighbor u-u and u-s lattice units, respectively, and e^0_{ss} and γ are the model parameters characterizing the interaction between nearest-neighbor s-s lattice units. Here we point out that very small change in the values of these model parameters may result in:
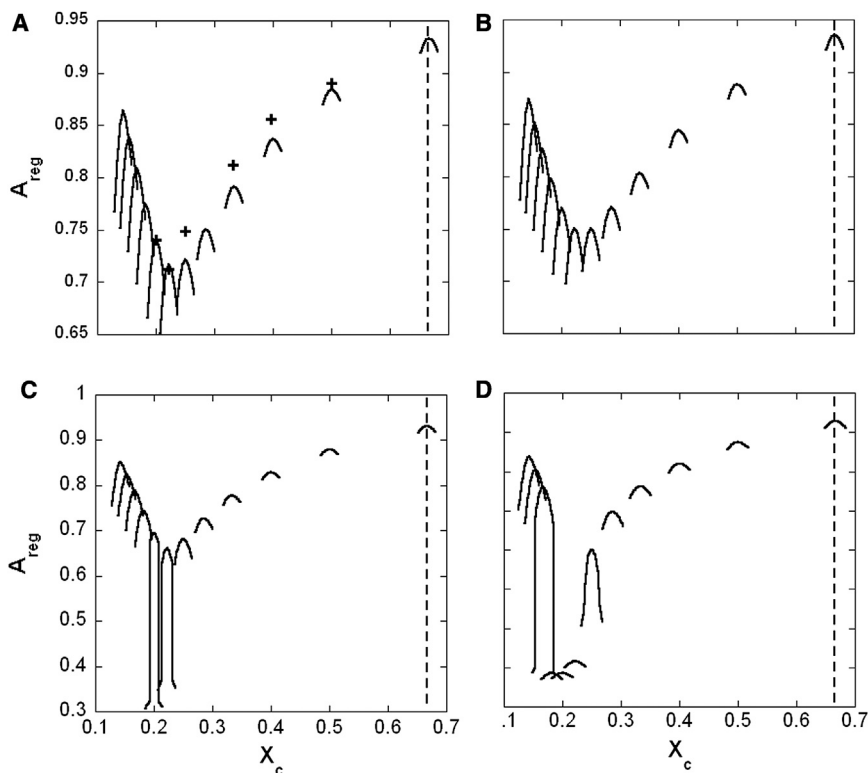
FIGURE 2 Proportion of regularly packed membrane area. Regular area fraction, A_{reg}, is plotted against the cholesterol mole fraction, X_c. (*Plus sign*) Measured local maxima of the regular area fraction (15,16). (*Solid lines*) Curve of calculated regular area fractions. (*Dashed line*) Cholesterol precipitates from the bilayer above this mole fraction (note this actual limit is characteristic for cholesterol/PC bilayers). Interaction energy parameters: (*A*) $e_{uu} = P_1[= -160.5 \text{ cal/mol}\cdot\text{Å}]$, $e_{us} = P_2[= -207 \text{ cal/mol}\cdot\text{Å}]$, $e_{ss}^0 = P_3[= -303.53 \text{ cal/mol}\cdot\text{Å}]$ and $\gamma = P_4[= -10952.48 \text{ cal}\cdot\text{Å/(mol)}]$; (*B*) $e_{uu} = P_1 \cdot 1.008$, $e_{us} = P_2 \cdot 1.008$, $e_{ss}^0 = P_3 \cdot 1.008$ and $\gamma = P_4 \cdot 1.008$; (*C*) $e_{uu} = P_1 \cdot 0.992$, $e_{us} = P_2 \cdot 0.992$, $e_{ss}^0 = P_3 \cdot 0.992$ and $\gamma = P_4 \cdot 0.992$; (*D*) $e_{uu} = P_1 \cdot 0.984$, $e_{us} = P_2 \cdot 0.984$, $e_{ss}^0 = P_3 \cdot 0.984$ and $\gamma = P_4 \cdot 0.984$.

1. Considerable sharpening of certain peaks, while the local maxima of the A_{reg} curves practically do not change, or
2. Considerable drop in the local maxima of the A_{reg} curves.

When the absolute value of each interaction parameter is increased by only 0.8%, the character of the calculated A_{reg} curves does not change; however, each curve slightly shifts toward higher A_{reg} values (see Fig. 2 B). On the other hand, when the absolute value of each interaction parameter is decreased by only 0.8%, the peaks at $M = 7$ and 8 become particularly sharp—but we do not see considerable drop in the local maxima of the A_{reg} curves (see Fig. 2 C). We point out below that each extremely sharp peak represents two first-order transitions, i.e., from fluid to superlattice (at $X_c < X^M_{cr}$) and from superlattice to fluid phase (at $X_c > X^M_{cr}$). With further weakening of the lateral interaction by another 0.8%, the peak heights at $M = 7$, 8, and 9 drop considerably, i.e., at the respective cholesterol mole fractions, ~60% of the bilayer is in fluid phase (see Fig. 2 D).

At $M = 6$ we get a moderately sharp peak. As it will be pointed out below, this peak represents two continuous transitions (or close to second-order phase transitions): from fluid to superlattice (at $X_c < X^6_{cr}$) and from superlattice to fluid phase (at $X_c > X^6_{cr}$). In general, by weakening the lateral interactions first, the A_{reg} values are continuously decreasing at every X_c then sudden decreases appear at midvalues of M (e.g., 7 and 8). At these sudden changes, first-order phase transitions take place either from fluid to superlattice or from superlattice to fluid phase. Upon further

decreasing the interactions, the fluid phase will be present everywhere at midvalues of M, whereas at lower as well as higher M values, A_{reg} suddenly increases through first- (or second-) order transitions into the superlattice phase. Note that in our examples we uniformly lowered the lateral interaction energy parameters. At nonuniform lowering of the parameter values one may expect changes in the details, whereas the above-described general trend would remain the same. The finding that changing the interaction energy parameters can alter the shape and magnitude of the A_{reg} peak, but not the peak maximum position, provides an explanation for why, in experimental studies of sterol superlattices (3,4,6,12), a biphasic change in membrane properties was observed almost always at X^M_c but the shape and depth (or height) of the biphasic change may vary from experiment to experiment.

Small continuous biphasic changes in A_{reg}

In Fig. 2, the typical peaks show small (1–10%) continuous changes in the A_{reg} value. The peak belonging to $M = 7$ in Fig. 2 A is examined in Fig. 3. The change of $\langle X^s_c \rangle$ versus X_c (Fig. 3 B) is similar to the A_{reg} versus X_c function (Fig. 3 A). To create these curves, we have to calculate and analyze the free energy curves (i.e., to find the global minima of the curves) at several cholesterol mole fractions that are close to the critical mole fraction, X^7_{cr}. For example, in Fig. 3 B, arrows point to the X_c values where the
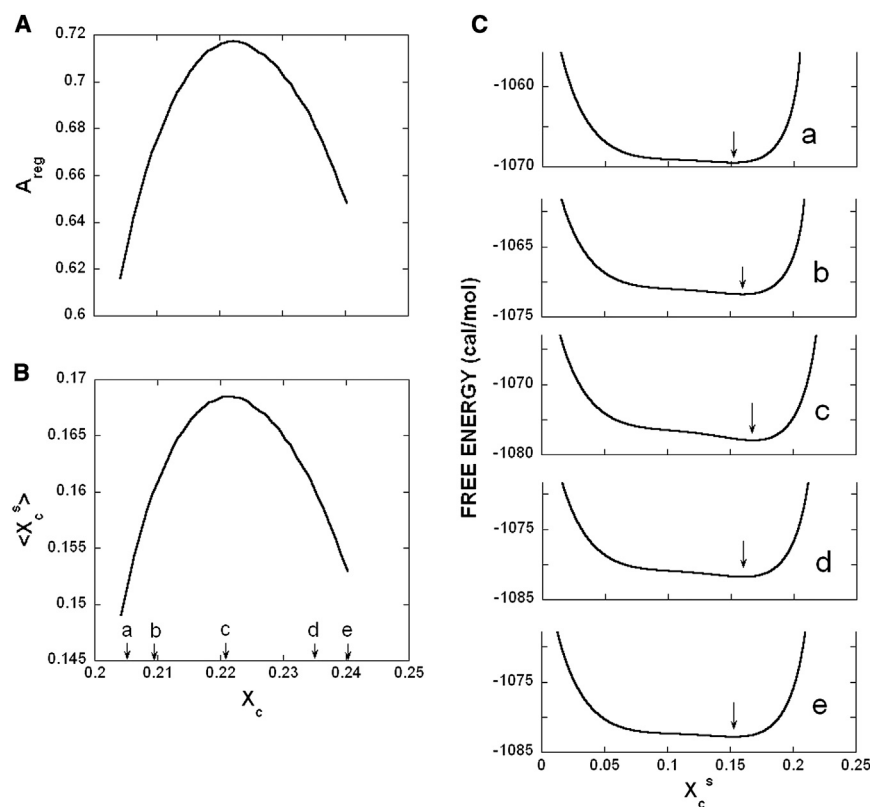
A

B

C

FIGURE 3 Analysis of the peak at $M = 7$ in Fig. 2 *A*. (*A*) Regular area fraction, A_{reg} is plotted against the cholesterol mole fraction, X_c. (*B*) The most probable X^s_c ($\cong \langle X^s_c \rangle$ maximum term approximation (17)) is plotted against the cholesterol mole fraction, X_c. (*Arrows*) X_c values where the free energy functions were calculated in panel *C*. (*C*) Five free energy functions are calculated at the following five cholesterol mole fractions: (*a*) $X_c = 0.2052$; (*b*) $X_c = 0.2092$; (*c*) $X_c = X^7_{cr} = 0.222$; (*d*) $X_c = 0.2352$; and (*e*) $X_c = 0.2402$. (*Solid arrow*) Global minimum of the free energy function.

respective, calculated free energy functions are shown in Fig. 3 *C*. In Fig. 3 *C*, arrows show the global minimum of each free energy function. According to the maximum term approximation (17), the X^s_c value at the global minimum of the free energy function defines the thermodynamic average (or the equilibrium value) $\langle X^s_c \rangle$ that is plotted in Fig. 3 *B*. Then, by substituting the $\langle X^s_c \rangle$ value into Eq. 3, one can get A_{reg} and plot Fig. 3 *A*. Along the investigated region of the cholesterol mole fraction (from $X_c = 0.2052$ to $X^7_{cr} = 0.222$), there is a continuous small increase in the proportion of the superlattice structure, while from the critical mole fraction (from X^7_c to $X_c = 0.2402$), the opposite trend can be observed.

First-order phase transitions

In Fig. 2 *C* at $M = 7$ and 8, the peak shows large (~60%) sudden changes in the A_{reg} value. The peak at $M = 7$ in Fig. 2 *C* is further examined, and the results are shown in Fig. 4. The change of $\langle X^s_c \rangle$ versus X_c (Fig. 4 *B*) is similar to the A_{reg} versus X_c function (Fig. 4 *A*). To create the curves in Fig. 4, *A* and *B*, we have to calculate and analyze the free energy curves (i.e., to find the global and local minima of the curves) at several cholesterol mole fractions that are close to the critical mole fraction, X^7_{cr}. For example, in Fig. 4 *B*, arrows point to the X_c values where the free energy functions are calculated and shown in Fig. 4 *C*. The A_{reg} peak is steepest at $X_c = 0.213$ and $X_c = 0.232$. At these mole fractions,

the free energy function has double global minima. At $X_c < 0.213$, the minimum at the lower X^s_c value is the global minimum of the free energy function (see *b* in Fig. 4 *C*), defining the equilibrium structure where fluid phase dominates.

However, when the cholesterol mole fraction becomes larger than 0.213, the minimum at the higher X^s_c value becomes the global minimum of the free energy function (see *c* in Fig. 4 *C*), defining the equilibrium structure where the superlattice phase dominates. Passing through the transition mole fraction, $X_c = 0.213$, the global minimum at the lower X^s_c value becomes the local minimum and the fluid-like system belonging to this local minimum becomes metastable. As a result of thermal fluctuations, sudden, cooperative transition may take place from the metastable to stable state (i.e., where the superlattice phase dominates) of the system. The metastable states of the system are marked by dotted lines in Fig. 4, *A* and *B*. Upon further increasing the cholesterol mole fraction the local minimum of the free energy function disappears and the metastable state of the system ceases to exist (see *d* in Fig. 4 *C*). The highest proportion of the superlattice phase is at the critical mole fraction, $X^7_{cr} = 0.222$. The reverse of the above-described first-order phase transition can be induced by further increasing the cholesterol mole fraction from $X_c = 0.222$ to $X_c = 0.2372$.

We note that the analysis of the extremely sharp peak at $M = 8$ in Fig. 2 *C* revealed two consecutive first-order phase
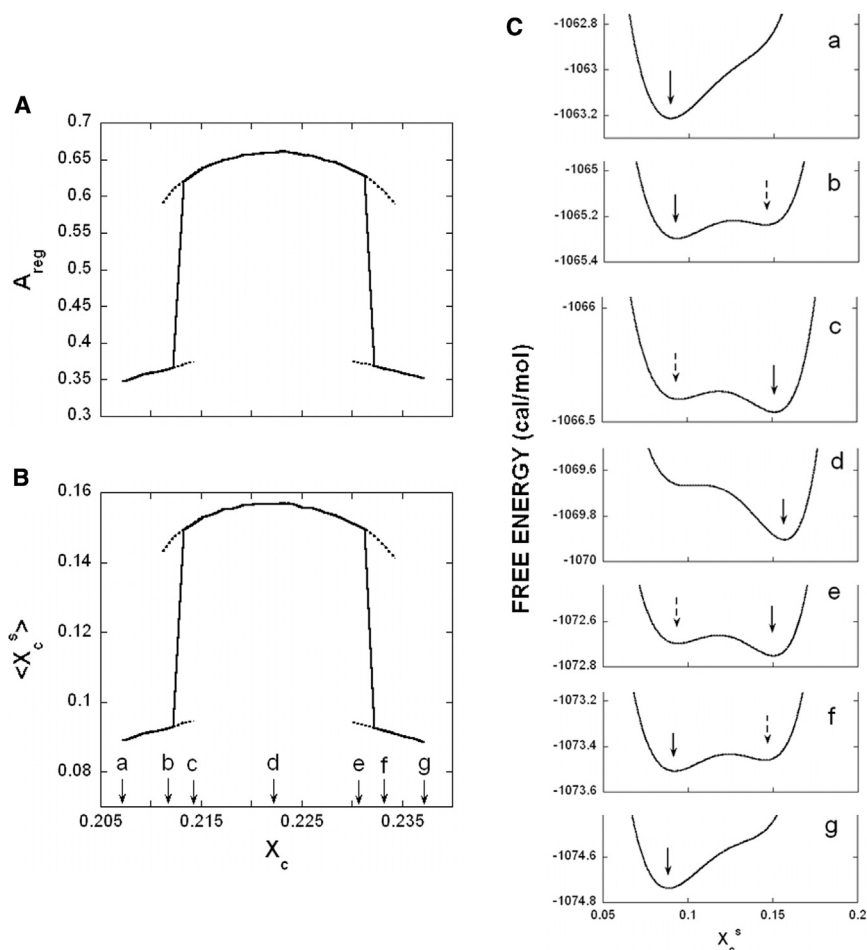
FIGURE 4 Analysis of the extremely sharp peak at $M = 7$ in Fig. 2 C. (A) Regular area fraction, A_{reg}, is plotted against the cholesterol mole fraction, X_c. (Solid and dotted lines) Stable and metastable system, respectively. (B) The most probable X^s_c ($\cong \langle X^s_c \rangle$ maximum term approximation (17)) is plotted against the cholesterol mole fraction, X_c (solid line). (Dotted line) Metastable system. (Arrows) X_c values where the free energy functions were calculated and presented in panel C. (C) Seven free energy functions are calculated at the following seven cholesterol mole fractions: (a) $X_c = 0.2072$; (b) $X_c = 0.2117$; (c) $X_c = 0.2142$; (d) $X_c = X^7_{cr} = 0.222$; (e) $X_c = 0.2307$; (f) $X_c = 0.2332$; and (g) $X_c = 0.2372$. (Solid and dashed arrows) Global and local minimum of the free energy function, respectively.

transitions similar to the ones found in the case of the peak at $M = 7$.

Continuous phase change

In Fig. 2 D at $M = 6$, the peak shows a large (~40%) continuous change in the A_{reg} value. This peak is examined in detail, and the results are presented in Fig. 5. Again the change of $\langle X^s_c \rangle$ versus X_c (Fig. 5 B) is similar to the A_{reg} versus X_c function (Fig. 5 A). To create the curves in Fig. 5, A and B, we have to calculate and analyze the free energy curves at several cholesterol mole fractions that are close to the critical mole fraction, X^6_{cr}. For example, in Fig. 5 B, arrows point to the X_c values where the free energy functions are calculated and presented in Fig. 5 C. In Fig. 5 C, arrows show the global minimum of the free energy function. The A_{reg} peak is steepest at $X_c = 0.238$ and $X_c = 0.262$. At these mole fractions, the free energy function has broad, almost flat minimum (Fig. 5 C, panels b and d). At $X_c < 0.238$, the global minimum of the free energy function (Fig. 5 C, panel a) defines an equilibrium structure where fluid phase dominates.

However, when the cholesterol mole fraction becomes larger than 0.238, the global minimum of the free energy

function is at a considerably higher X^s_c value (Fig. 5 C, panel c) defining an equilibrium structure where the superlattice phase dominates. In contrast to the first-order phase transition, in this case, the system is in stable state throughout the phase change, and it shows particularly large fluctuations at the transition mole fraction where the free energy function is almost flat. These are characteristic to a continuous phase change (or a close to second-order phase transition). The highest proportion of the superlattice phase is at the critical mole fraction, $X^6_{cr} = 0.25$. Upon further increasing the cholesterol mole fraction, the opposite continuous phase change takes place at $X_c = 0.262$.

In this article, the values of every model parameter controlling the lateral interactions between nearest-neighbor lattice units was slightly and simultaneously decreased by the same rate, i.e.: by 0.8%. As a result, sudden concentration-induced phase changes took place in the range of cholesterol mole fraction from 0.18 to 0.26. In the future, it would be interesting to investigate the phase changes when the values of the model parameters are decreased by different rates.

The applicability of the version of the model discussed in this article is restricted to cholesterol mole fractions that are close to any of the critical mole fractions. At $M > 6$, the
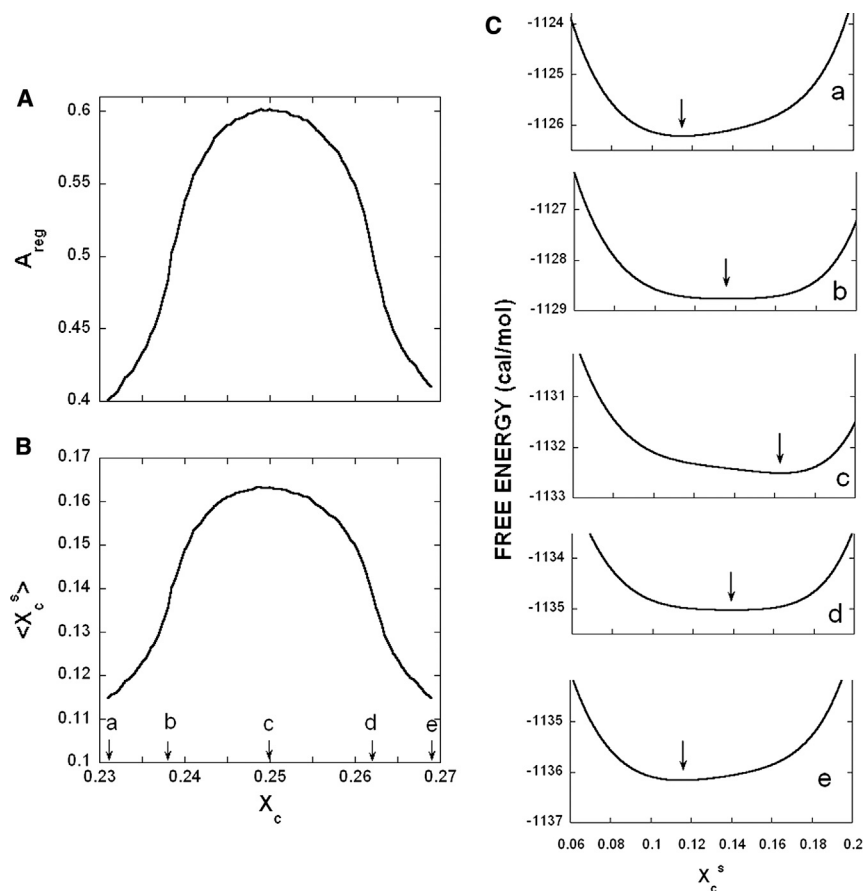
FIGURE 5 Analysis of the peak at $M = 6$ in Fig. 2 D. (A) Regular area fraction, A_{reg}, is plotted against the cholesterol mole fraction, X_c. (B) The most probable X^s_c ($\cong \langle X^s_c \rangle$ maximum term approximation (17)) is plotted against the cholesterol mole fraction, X_c. (Arrows) X_c values where the free energy functions were calculated in panel C. (C) Five free energy functions are calculated at the following five cholesterol mole fractions: (a) $X_c = 0.231$; (b) $X_c = 0.238$; (c) $X_c = X^6_{cr} = 0.25$; (d) $X_c = 0.262$; and (e) $X_c = 0.269$. (Solid arrow) Global minimum of the free energy function.

critical mole fractions are so close to each other that the model is applicable at any cholesterol mole fractions. However, at $M \le 6$, the critical mole fractions are farther from each other while the model is applicable only close to these critical mole fractions, i.e., there are gaps where the model is not applicable. To reveal the phase properties in the whole range of the cholesterol mole fractions, one has to generalize the statistical mechanical model. It is important to note that the available nystatin fluorescence measurements (15) do not show sharp changes in A_{reg} at $M \le 6$.

In the light of the theoretical results obtained from this work and the experimental detection of biphasic changes in membrane properties at X^M_{cr} (3–5,15,16), the phase diagram of cholesterol/phospholipid mixtures looks much more complicated than it was believed earlier, based on rather limited calorimetric, NMR, and micromechanical data (see references in Sugár and Chong (13)).

CONCLUSIONS

Here concentration-induced phase transition properties of our recently developed statistical mechanical model of cholesterol/phospholipid mixtures are investigated (13). Slight ($<1\%$) decrease in the model parameter values, controlling the lateral interaction energies, reveals the existence of a series of first- or second-order phase transitions. By weakening the lateral interactions first, the proportion of the ordered (i.e., superlattice) phase is slightly and continuously decreasing at every cholesterol mole fraction. Then sudden decreases appear at the 0.18–0.26 range of cholesterol mole fractions. The sudden changes represent first- or second-order concentration-induced phase transitions from fluid to superlattice and from superlattice to fluid phase. Sudden changes like these were detected by us at 0.2, 0.222, and 0.25 cholesterol mole fractions in ergosterol/DMPC mixtures (15).

By further decreasing the lateral interactions, fluid phase will dominate throughout the 0.18–0.26 interval, while outside this interval, sudden changes in A_{reg} may appear. Our results demonstrate that very small changes in the lateral interaction energies (that can be triggered by physical and/or chemical perturbations) may result in considerable changes in the phase properties of the cholesterol/phospholipid mixtures, which may have important functional consequences. In view of the fact that the temperature and pressure in cell membranes are largely invariant under physiological conditions, the lipid composition-induced phase transitions as specified here should have far more important biological implications than temperature- or pressure-induced phase transitions. More studies on this subject are in demand.

REFERENCES

1. Ipsen, J. H., G. Karlström, …, M. J. Zuckermann. 1987. Phase equilibria in the phosphatidylcholine-cholesterol system. *Biochim. Biophys. Acta.* 905:162–172.

2. Huang, T.-H., C. W. B. Lee, …, R. G. Griffin. 1993. A ^{13}C and ^{2}H nuclear magnetic resonance study of phosphatidylcholine/cholesterol interactions: characterization of liquid-gel phases. *Biochemistry.* 32:13277–13287.

3. Chong, P. L.-G., and M. Olsher. 2004. Fluorescence studies of the existence and functional importance of regular distributions in liposomal membranes. *Soft Materials.* 2:85–108.

4. Chong, P. L.-G., W. Zhu, and B. Venegas. 2009. On the lateral structure of model membranes containing cholesterol. *Biochim. Biophys. Acta.* 1788:2–11.

5. Somerharju, P., J. A. Virtanen, …, M. Hermansson. 2009. The superlattice model of lateral organization of membranes and its implications on membrane lipid homeostasis. *Biochim. Biophys. Acta.* 1788:12–23.

6. Chong, P. L.-G. 1994. Evidence for regular distribution of sterols in liquid crystalline phosphatidylcholine bilayers. *Proc. Natl. Acad. Sci. USA.* 91:10069–10073.

7. Virtanen, J. A., M. Ruonala, …, P. Somerharju. 1995. Lateral organization of liquid-crystalline cholesterol-dimyristoylphosphatidylcholine bilayers. Evidence for domains with hexagonal and centered rectangular cholesterol superlattices. *Biochemistry.* 34:11568–11581.

8. Huang, J. 2002. Exploration of molecular interactions in cholesterol superlattices: effect of multibody interactions. *Biophys. J.* 83:1014–1025.

9. Virtanen, J. A., P. Somerharju, and P. K. J. Kinnunen. 1988. Prediction of patterns for the regular distribution of soluted guest molecules in liquid crystalline phospholipid membranes. *J. Mol. Electron.* 4:233–236.

10. McConnell, H. M., and A. Radhakrishnan. 2003. Condensed complexes of cholesterol and phospholipids. *Biochim. Biophys. Acta.* 1610:159–173.

11. Radhakrishnan, A., and H. M. McConnell. 1999. Condensed complexes of cholesterol and phospholipids. *Biophys. J.* 77:1507–1517.

12. Venegas, B., I. P. Sugár, and P. L.-G. Chong. 2007. Critical factors for detection of biphasic changes in membrane properties at specific sterol mole fractions for maximal superlattice formation. *J. Phys. Chem. B.* 111:5180–5192.

13. Sugár, I. P., and P. L.-G. Chong. 2012. A statistical mechanical model of cholesterol/phospholipid mixtures: linking condensed complexes, superlattices, and the phase diagram. *J. Am. Chem. Soc.* 134:1164–1171.

14. Sugár, I. P. 2008. On the inner structure and topology of clusters in two-component lipid bilayers. Comparison of monomer and dimer Ising models. *J. Phys. Chem. B.* 112:11631–11642.

15. Wang, M. M., I. P. Sugár, and P. L.-G. Chong. 1998. Role of the sterol superlattice in the partitioning of the antifungal drug nystatin into lipid membranes. *Biochemistry.* 37:11797–11805.

16. Wang, M. M., M. Olsher, …, P. L.-G. Chong. 2004. Cholesterol superlattice modulates the activity of cholesterol oxidase in lipid membranes. *Biochemistry.* 43:2159–2166.

17. Hill, T. L. 1987. Statistical Mechanics: Principles and Selected Application. Dover, Mineola, New York.